

REPORT DOCUMENTATION PAGE

Form Approved
OMB No. 0704-0188

Public reporting burden for this collection of information is estimated to average 1 hour per response, including the time for reviewing instructions, searching existing data sources, gathering and maintaining the data needed, and completing and reviewing the collection of information. Send comments regarding this burden estimate or any other aspect of this collection of information, including suggestions for reducing this burden, to Washington Headquarters Services, Directorate for Information Operations and Reports, 1215 Jefferson Davis Highway, Suite 1204, Arlington, VA 22202-4302, and to the Office of Management and Budget, Paperwork Reduction Project (0704-0188), Washington, DC 20503.

1. AGENCY USE ONLY (Leave blank)	2. REPORT DATE	3. REPORT TYPE AND DATES COVERED	
	July 29, 1995	Technical Report / June 1994-May 1995	
4. TITLE AND SUBTITLE		5. FUNDING NUMBERS	
Measurement of Thru-Space Dipole-Dipole Coupling from Shifts in Vibrational Frequencies for a Stlibazolium derivative Embedded in a Self-Assembled Monolayer		Grant # N00014-90-J-1167 R&T Code 4133019	
6. AUTHOR(S)			
John Pope and Daniel A. Buttry			
7. PERFORMING ORGANIZATION NAME(S) AND ADDRESS(ES)		8. PERFORMING ORGANIZATION REPORT NUMBER	
Department of Chemistry, University of Wyoming Laramie, WY 82071-3838			
9. SPONSORING/MONITORING AGENCY NAME(S) AND ADDRESS(ES)		10. SPONSORING/MONITORING AGENCY REPORT NUMBER	
Office of Naval Research Chemistry Division 800 N. Quincy Street Arlington, VA		Technical Report #26	
11. SUPPLEMENTARY NOTES			
Prepared for publication in Langmuir			
12a. DISTRIBUTION/AVAILABILITY STATEMENT		12b. DISTRIBUTION CODE	
This document has been approved for public release and sale; its distribution is unlimited			
13. ABSTRACT (Maximum 200 words)			
<p>Abstract: Self-assembled monolayers (SAM's) were produced from the spontaneous adsorption of a thiol-bearing stilbazolium derivative and dodecanethiol. A range of mole fractions in the solutions from which these SAM's were produced was used to give monolayers with varying amounts of the stilbazolium derivative and the n-alkyl thiol. The relatively large dipole moment of the stilbazolium derivative leads to dipole-dipole coupling between these derivatives, as demonstrated from shifts in the vibrational frequencies of certain normal modes of this compound. The magnitude and surface coverage dependence of these shifts indicate that this dipole-dipole coupling is due to a through-space, electrostatic interaction between the immobilized dipoles. This study comprises the first experimental demonstration of this phenomenon in monolayers supported on solid substrates.</p>			
DTIC QUALITY INSPECTED 5			
14. SUBJECT TERMS		15. NUMBER OF PAGES	
monolayer, infrared spectroscopy, dipole-dipole coupling		25	
		16. PRICE CODE	
17. SECURITY CLASSIFICATION OF REPORT	18. SECURITY CLASSIFICATION OF THIS PAGE	19. SECURITY CLASSIFICATION OF ABSTRACT	20. LIMITATION OF ABSTRACT
unclassified	unclassified	unclassified	UL

19951120030

OFFICE OF NAVAL RESEARCH

GRANT #: N00014-90-J-1167

R&T Code: 4133019

Technical Report No. 26

Measurement of Through-Space Dipole-Dipole Coupling from Shifts in Vibrational Band Frequencies for a Stilbazolium Derivative Embedded in a Self-Assembled Monolayer

John M. Pope and Daniel A. Buttry

Prepared for publication

in

Langmuir.

Department of Chemistry
University of Wyoming
Laramie, WY 82071-3838

July 29, 1995

Reproduction in whole, or in part, is permitted for any purpose of the
United States Government.

This document has been approved for public release and sale; its
distribution is unlimited.

Measurement of Through-Space Dipole-Dipole Coupling from Shifts in Vibrational Band Frequencies for a Stilbazolium Derivative Embedded in a Self-Assembled Monolayer

John M. Pope and Daniel A. Buttry*

Department of Chemistry

University of Wyoming

Laramie, WY 82071-3838

Abstract: Self-assembled monolayers (SAM's) were produced from the spontaneous adsorption of a thiol-bearing stilbazolium derivative and dodecanethiol. A range of mole fractions in the solutions from which these SAM's were produced was used to give monolayers with varying amounts of the stilbazolium derivative and the n-alkyl thiol. The relatively large dipole moment of the stilbazolium derivative leads to dipole-dipole coupling between these derivatives, as demonstrated from shifts in the vibrational frequencies of certain normal modes of this compound. The magnitude and surface coverage dependence of these shifts indicate that this dipole-dipole coupling is due to a through-space, electrostatic interaction between the immobilized dipoles. This study comprises the first experimental demonstration of this phenomenon in monolayers supported on solid substrates.

Introduction

The spontaneous assembly of molecules at surfaces provides a simple, yet powerful, method of constructing interfaces with well-defined structure and composition.¹ The ease with which such self-assembled monolayers (SAM's) can be produced and the wide range of molecular entities that can be introduced into them has resulted in a number of studies of the behavior of redox or chromophoric species that have been immobilized in such assemblies. For example, we have employed this approach to produce SAM's that contain a fluorescent probe to allow for the *in situ* measurement of the electric field at the electrode-solution interface.² Those monolayers were comprised of a mixture of the thiol-bearing probe species (a stilbazolium derivative, compound I, shown in Figure 1) and various n-alkyl thiols. While characterizing how the structure and composition of these monolayers depend on loading conditions using infrared spectroscopy, contact angle goniometry, and electrochemistry, we have observed a monotonic dependence of the positions of certain vibrational bands of the probe on the mole fraction of the probe in the two-component SAM's. We believe this effect is a manifestation of interadsorbate dipole-dipole coupling between the dipolar probe species. Dipole-dipole coupling has been observed in other types of adsorbed monolayers (see below). However, previous observations have been limited to cases in which the dipolar adsorbates are electronically coupled to the substrate,³⁻⁷ which considerably complicates the interpretation of the shifts in the vibrational bands. In this contribution, we report, to our knowledge, the

first observation of dynamic dipolar coupling in a system where the adsorbate is electronically insulated from the surface.

The classic example of an adsorbed dipolar species that demonstrates interadsorbate dipolar coupling is carbon monoxide adsorbed onto various metals, such as Pt. This dipolar coupling results in significant changes in the vibrational spectrum of the adsorbed CO, with the most evident and most widely studied effect being a shift in the band position that is strongly dependent on the surface coverage of the adsorbed CO. Reflection-absorption Fourier transform infrared spectroscopy (RA-FTIR) and other vibrational spectroscopies suitable for interrogating interfacial species have been used extensively to study this phenomenon³⁻⁷. Various models to explain these shifts have been postulated.⁴ They can be grouped into two general categories: inductive coupling models that involve the metal substrate in the coupling mechanism and a lateral, through-space, electrostatic dipole-dipole coupling model. The former models include coupling through the metal (suggested by Grimley⁸ and developed by Cotton and Krahanzel⁹ to describe the vibrational coupling between multiple CO ligands in metal carbonyl species, and later adapted to CO monolayers on metal surfaces¹⁰), coupling to the dipole images in the metal, and changes in the electronic structure of the metal and/or adsorbate due to adsorbate binding.⁴ The so-called vibrational coupling model¹⁰ provides an example of how these interactions can affect the vibrational spectrum of an adsorbate. In this model, changes in the atomic coordinates of one adsorbate (such as take place during a vibration) lead to changes in the bond strength of an adjacent adsorbate. This type of interaction has been postulated¹⁰ to be mediated through the electronic structure of the metal, so it does not necessarily follow the r^{-3} distance dependence expected for through-space dipole-dipole coupling.⁴ It predicts a splitting of the CO vibrational mode into a symmetric, ir-active mode and an asymmetric, ir-inactive mode, which results in the observation of a single vibrational mode in the infrared spectrum that shifts in frequency as a function of surface coverage.¹⁰ Models of this type have been developed largely because the magnitudes of the band shifts observed for adsorbates such as CO on Pt are much larger than those predicted from through-space dipole-dipole coupling models.⁴

Inductive coupling of the type described above requires that the adsorbate molecules be in electronic communication with the metal substrate. However, in SAM's of the type described here, direct interaction of the probe orbitals with the metal is precluded by the intervening alkyl chains. Thus, the through-space, dipole-dipole coupling model would seem to be a better choice to describe this system. This model was first suggested in 1956 by Eischens, Francis, and Pliskin¹¹ (although earlier Decius considered dipolar coupling to explain isotope effects in the spectra of carbonate and nitrate crystals¹²) and later expanded upon by Hammaker, Francis, and Eischens in 1965,¹³ with some revision in the intervening years.¹⁴⁻¹⁶ In this model, lateral, purely electrostatic coupling between oscillating dipoles leads to changes in the bond strength of a given adsorbate and to splitting of the vibrational modes, just as

is the case for the vibrational coupling model described above. (However, note that the nature of the coupling is different for these two models.) Again, only one of the bands is observed in the infrared spectrum, and its frequency is increased as the magnitude of the coupling interaction is increased. Since dipolar coupling comprises a simple dipole-dipole electrostatic interaction, this model requires a r^{-3} distance dependence for the magnitude of the interaction, which leads to a predictable dependence of the coupling interaction on surface coverage. The treatment by Hammaker et al.¹³ resulted in a prediction of the dependence of the vibrational frequency on several parameters. This prediction is embodied in equation 1 below:

$$\delta(\theta) = v^2 - v_0^2 = \frac{a^2}{4\pi^2 c^2 M_r \epsilon_0} \sum_{j=2}^N R_j^{-3} \quad (1)$$

where v is the frequency (in cm^{-1}) of the band in the presence of perturbing dipolar fields, v_0 is the singleton frequency of the same mode (i.e. the frequency of an isolated molecule), a is the change in dipole moment with normal coordinate ($= \partial\mu/\partial Q$), c is the speed of light, M_r is the reduced mass of the oscillator, ϵ_0 is the permittivity of vacuum, and R_j is the distance from the single molecule to the perturbing molecule, summed over all the molecules in the monolayer. The sum over R^{-3} was shown to be approximately linear with surface coverage for a variety of possible surface structures (i.e. different single crystal surfaces).¹³ Thus, the quantity on the left-hand side of the equation, $\delta(\theta)$, is usually plotted against the surface coverage, with linear behavior being taken as indicative of dipolar coupling. Note that this requires random population of the surface sites as coverage is increased. Deviations from linear behavior have frequently been interpreted as arising from clustering or island formation.¹⁷

It is especially significant that the dipolar coupling model predicts that the magnitude of the coupling interaction depends on the square of the dipole moment change during the vibration, i.e. on $(\partial\mu/\partial Q)^2$, where μ is the dipole moment and Q is the normal coordinate. Thus, only those modes that significantly change μ will lead to strong coupling. The implication is that, for complex molecules such as I, vibrational band shifts due to dipolar coupling will only be observed for those modes whose vibrational motion significantly changes the dipole moment of the molecule. As will be seen below, this prediction is born out in the behavior of the SAM's described here. Finally, note that $(\partial\mu/\partial Q)^2$ can be obtained from the infrared spectrum¹⁰ of compound I (see below). This allows one to calculate the expected value of $\delta(\theta)$ using equation 1 and to compare it to the experimentally obtained value, thereby directly testing whether the dipolar coupling model is applicable in this case.

Experimental

ion For	RA&I	<input checked="" type="checkbox"/>
seed	B	<input type="checkbox"/>
ration	C	<input type="checkbox"/>
By		
Distribution/		
Availability Codes		
Dist	Avail and/or Spec	

To make the dye precursor, hemicyanine, a published route¹⁸ was followed where N,N-p-bromo(dimethyl) aniline (12.000 g, 0.06 moles, Aldrich, 24,295-0, 99%), Pd(II) acetate (0.1355 g, 0.6 mmoles, Aldrich, 20,586-9, 98%), tri-o-tolyl phosphine (0.3654 g, 1.2 mmoles, Aldrich, 28,782-2, 97%), and 4-vinyl pyridine (8.1 ml, 0.075 moles, Aldrich) were dissolved in dry triethylamine (Mallinckrodt OR) and placed in a 100 ml reaction vessel (medium walled). The vessel was heated in an oil bath at 110° C for 72 hours under a 100 torr N₂ atmosphere. After reaction, the solids were removed by dissolution (over 4 hours) in ca. 2 liters of CH₂Cl₂ and a small amount of H₂O. A small amount of green solid was filtered off. A water/chloroform extraction was performed on the solution; overnight equilibration was necessary for a good initial separation of layers. The water layer was washed twice with chloroform, the washings of which were added to the chloroform layer. The chloroform layer was washed once with water and dried over anhydrous MgSO₄. The solvent was removed by rotary evaporation and the solid was dried overnight at 10⁻⁴ torr. The yellow solid was recrystallized from a 2:1 mixture of methanol and acetone (1.5 liters, total) and dried at 10⁻⁴ torr overnight for a 56% yield.

To derivatize the precursor, the hemicyanine pyridine group was quaternized with a short alkyl chain. Hemicyanine (1 g, 4.5 mmoles) was dissolved in 200 ml of warm toluene (EM Omnisolv, HPLC grade). Tetrabutylammonium iodide (58 mg, 0.16 mmoles, Aldrich, 14077-5, 98%) was added to catalyze the reaction. 1,3-dibromopropane (2 ml, 20 mmoles, Aldrich, 12,590-3, 99%) was added to the reaction mixture which was subsequently heated at reflux under N₂ for 22 hours. The red precipitate was filtered, washed with copious amounts of hot toluene and cold diethyl ether (Mallinckrodt Analytical Reagent), and dried at 0.0001 torr overnight. (60% yield) [¹H NMR (270 MHz) δ 4.5 (t, 2 H), 3.6 (t, 2 H), 3.0 (s, 6 H)].

The 1PAS3Br•Br⁻ dye (e.g. bromide salt of hemicyanine quaternized with a 3 carbon chain ending with a bromine atom) was converted to the thiol compound (1PAS3SH•Br⁻) in a two-step process. First, the bromide was displaced with deprotonated thioacetic acid. Cs₂CO₃ (241 mg, 0.74 mmoles, 1.05 eq., Aldrich, 20212-6, 99.9%) was dissolved in dry, degassed methanol (50 ml), to which thioacetic acid (0.1 ml, 1.48 mmoles) was added slowly. After stirring, this mixture was added to a solution of 1PAS3Br•Br⁻ (600 mg, 1.41 mmoles) in dry, degassed methanol (150 ml) and purged with N₂ gas. The reaction mixture was refluxed under N₂ for 25 hours, after which the solvent was removed by rotary evaporation to leave 767 mg total solids (of which 509 mg, or 1.21 mmoles, were the thioester derivatized dye). [¹H NMR (270 MHz) δ 4.5 (t, 2 H), 3.0 (s, 6 H), 2.9 (t, 2 H), 2.35 (s, 3 H), 2.15 (p, 2 H)]. Second, the thioester moiety was cleaved to the thiol group following published procedures.¹⁹ The resultant 1PAS3SH•Br⁻ dye was precipitated from methanol by adding a saturated solution of NaNO₃ to give 1PAS3SH•NO₃⁻ (shown in Figure 1).

Flat gold substrates were prepared from gold-coated microscope slides (1x3 inches, Fisher, 12550-A) which were immersed overnight in a cleaning bath of NoChromix (GOORX Laboratories, Inc.) dissolved in H₂SO₄ (VWR, ACS Reagent, VW-6840-3, 95-98%), after which they were evaporatively coated with ca. 75 Å of chromium and then ca. 2000 Å of gold using an Edwards Coating System (E306A). Prior to coating, the slides were plasma etched for at least 10 minutes. The coating process was monitored using an Edwards Film Thickness Monitor (Edwards High Vacuum, Inc., model FTM4) and controlled so that the deposition rate of chromium was ca. 0.5-5 Å and of gold was ca. 1 Å per second. Slides were taken from the vacuum chamber and placed immediately into loading solutions.

All monolayers were loaded from solutions of thiol compounds of 1 mM *total* concentration in absolute methanol. To load a monolayer, a substrate was immersed in a freshly mixed solution, and, after 30 minutes, the substrate was removed from the solution and washed with copious amounts of absolute methanol and then diethyl ether. Samples were placed immediately into a dessicator (and subsequently stored there) with a fresh piece of Ag wire.

Contact angle measurements were taken on a NRL C. A. Goniometer (Ramé-Hart, Inc., model 100-00-115). Fresh de-ionized water was used in all measurements.

All *ex situ* FTIR spectra were taken on a Bomem MB-100 instrument using Lab Calc collection drivers (Galactic Industries) and were processed using Lab Calc PC-based software. The sample compartment was purged with dry N₂ blowoff from an in-house tank. External reflection spectra were collected from 1 x 3 inch gold-coated glass slides mounted in a Variable Reflectance Angle sample accessory (Harrick, Inc.) set at 80° using a HgCdTe liquid N₂-cooled detector. Incident radiation was p-polarized using a wire grid polarizer (SpectraTech). Apodization of all interferograms was done using a boxcar function. All data and background spectra were collected as single-beam spectra. Bulk were obtained in KBr pellets. 256 scans were taken at a resolution of 2 cm⁻¹.

Monolayers of perdeuterated hexadecane thiol on gold-coated glass slides were used as background samples.²⁰ This is a useful procedure that helps avoid spurious contamination of the Au electrode used as the background by virtue of the low surface energy and, consequentially, low level of surface contamination of the perdeuterated SAM. Deuterated hexadecane thiol was synthesized via the Mitsunobo route¹⁹ from deuterated n-hexadecanol (Cambridge Isotopes, 98%).

Absorption spectra of water and CO₂ changes in the purge atmosphere were created using single-beam spectra of identical background samples and were subtracted from the sample absorption spectra. Linear (manual) manipulation of peak intensities in the subtrahend absorption spectra was used to minimize water and CO₂ in the data absorption spectra.

Calculations of the vibrational spectrum of compound I were made using the Spartan quantum chemistry package (Spartan SGI version 4.0.3, Wavefunction, Inc., Irvine CA) at the AM1 level.

Results

Evaluation of the influence of dipolar coupling on the infrared spectrum of I requires knowledge of some of the vibrational band assignments for this compound. These assignments were made or confirmed based on a consideration of published band assignments (Table 1), semi-empirical calculations, and the results of the spectroscopic investigations of the monolayer samples. The transmission infrared spectrum of a bulk sample of 1PAS3SH is shown in Figure 2. The bands that are relevant to this discussion have frequencies at 1528 cm⁻¹, 1588 cm⁻¹, and 1640 cm⁻¹ (note that the large band at ca. 1460 cm⁻¹ is due to contamination of the sample by high vacuum grease). The bonds that make the primary contributions to the overall displacement for each band were determined from semi-empirical calculations. They are graphically depicted in Figure 3 and listed as follows. The band at 1528 cm⁻¹ has primary contributions from the asymmetric stretch of the two C-C bonds between the vinylic group and the two ring systems, with minor contributions (not shown) from the stretch of the amine nitrogen-aromatic carbon bond. As is obvious from Table I, some confusion exists in the literature about the assignment of the band at 1588 cm⁻¹. According to the calculations, the band at 1588 cm⁻¹ has primary contributions from the asymmetric stretch of the C=C bonds along the long axis of the molecule in the phenyl and pyridinium rings with minor contributions (not shown) from stretches of the amine nitrogen-aromatic carbon bond and the C-C bond between the vinyl group and the pyridinium ring. This assignment is favored because it agrees with both the observation of an intense peak in the infrared spectrum due to the large dipole moment change expected from this mode (i.e. this out-of-phase ring breathing vibration should lead to charge oscillation between the donor and acceptor ring systems, and, therefore, a large value of $\partial\mu/\partial Q$) as well as the large peak in the Raman spectrum²¹ due to the large polarizability change expected for this vibration (again, based on significant charge oscillation between the rings). In addition, this assignment agrees with the observation of a significant shift in the frequency of this band as a function of surface coverage due to dipole coupling (see below). The assignment of this band as the symmetric, vinylic C=C stretch by Shibasaki and Itoh is not consistent with the large intensity observed for this band in both the Raman and infrared spectra, so it was rejected. Finally, the band at 1640 cm⁻¹ has primary contributions from stretching of the vinylic C=C double bond with minor contributions (not

shown) from the adjoining single bonds and the two rings. This assignment is consistent with the low intensity of this band in the infrared spectrum. Note that with the exception of one problematic assignment for the 1588 cm^{-1} band²¹, there is general agreement on these band assignments in the literature.

Vibrational band assignments for the n-alkyl chains have been exhaustively studied both for the bulk phase materials and in monolayers. The pertinent bands and their frequencies and normal mode vectors are summarized in Table II.

Ex situ RA-FTIR spectra of six 1PAS3/C12 monolayers assembled from solutions of incrementally varied composition are shown in Figure 4. A salient feature of the spectra in Figure 4a is that the frequencies of the vibrational bands at 1528 cm^{-1} and 1588 cm^{-1} increase to 1529 cm^{-1} and 1596 cm^{-1} , respectively, as the mole fraction of I is increased from 0.10 to 0.95 in the loading solution. The area of these two peaks also increases considerably as the mole fraction of I in solution is increased, presumably due to than increase in the mole fraction of I on the surface. In the C-H region (Figure 4b), as the mole fraction of I in the loading solution increases from 0.1 to 0.95, the CH_2 band at 2850 cm^{-1} and the CH_3 band at 2878 cm^{-1} both decrease in area by ca. 50%, while the CH_3 band at 2965 cm^{-1} decreases in area by ca. 90%. Again, these changes in peak area aer consistent with an increase in the amount of I on the surface and a decrease in the amount of n-alkyl thiol as the mole fraction of I in the loading solution is increased. These changes in peak area accompanied by a shift in the $\nu_a(\text{CH}_2)$ band from 2919.5 cm^{-1} to 2921.5 cm^{-1} , perhaps indicating an slight decrease in the degree of order in the monolayer²⁰ as the n-alkyl thiols are replaced by I. However, it is significant that the peak position of this band is well below that expected²⁰ for a highly disordered, poorly oriented monolayer ($2924 - 2925\text{ cm}^{-1}$) for all mole fractions of I. This suggests that a significant fraction of the n-alkyl chains adopt a conformation and orientation in these monolayers similar to that observed in pure n-alkyl thiol SAM's, and, therefore, that the long axis of I is probably oriented substantially along the surface normal.

Figure 5 shows plots of the peak areas of the CH_2 band at 2850 cm^{-1} and of the 1588 cm^{-1} band of I versus the mole fraction of I in the loading solution. We take these peak areas as representative of the relative surface populations of the n-alkyl thiol and of compound I, respectively. Note, however, that I also contains CH_2 moieties, so the 2850 cm^{-1} peak area also contains contributions from the n-alkyl thiols. The concave upward plot for the 1588 cm^{-1} band and the concave downward plot for the 2850 cm^{-1} band are reminescent of data for mixed monolayers of n-alkyl thiols and thiol-bearing ferrocene derivatives that were studied by Rowe and Creager.²⁷ Our interpretation of these features as being indicative of preferential adsorption of the n-alkyl thiol compared to I is consistent with theirs.²⁷

Figure 6 shows a plot of the advancing contact angle for water on these monolayers as a function of the mole fraction of **I** in the loading solution. These data indicate that the SAM's that contain a large fraction of the n-alkyl thiol are quite hydrophobic, and that the hydrophobicity decreases as the n-alkyl thiol is replaced by **I**. These results are consistent with expectations that the dimethylamino group at the donor end of **I** would be less hydrophobic than an alkyl chain. It is worth noting that the trend in the contact angle very closely mirrors the change in the 1588 cm^{-1} peak area, suggesting that both quantities provide a good measure of the amount of **I** in the SAM. The fact that the contact angles are all fairly high suggests that the charged segment of **I** is not exposed at the SAM-water interface. Again, this suggests an orientation of the long axis of **I** along the surface normal, consistent with the arguments given above.

Discussion

The data in Figure 4 show that the frequencies of the 1588 cm^{-1} and 1528 cm^{-1} bands increase as the amount of **I** in the SAM is increased, with the former band increasing by 8 cm^{-1} and the latter by ca. 1 cm^{-1} over the range of mole fractions investigated. The dipolar coupling model¹³ suggests that a plot of δ versus R^3 should be linear if dipolar coupling is the primary source of the observed shifts in the vibrational bands. Geometrical analysis¹³ of the dependence of R^3 on surface coverage further suggests that, since R^3 is approximately linear with surface coverage, a plot of δ versus surface coverage should also be linear, given random occupancy of the surface sites (i.e. no islands or clusters of **I** are observed). Making such a plot requires knowledge of the surface coverage of **I** for each monolayer sample. To a first approximation, this can be obtained from the peak areas of either the 1528 cm^{-1} or 1588 cm^{-1} band as a function of the mole fraction of **I** in the loading solution. It is convenient to normalize these to the peak area at maximum coverage of **I**. We use the 1588 cm^{-1} band for this purpose because its greater area introduces less uncertainty into the values obtained from this procedure. Important assumptions inherent in this procedure are that the molar absorptivity of this band does not depend on the surface coverage of **I** (i.e. that dipolar coupling does not affect the molar absorptivity) and that the orientation of **I** also does not depend on the surface coverage of **I**, because orientational changes would lead to changes in the observed absorbances^{1,4,6,10,19}. The first assumption is supported by the theoretical analysis¹³, which indicates that the total integrated intensity of the band should not depend on coupling, and by the good agreement between the plots of both the 1588 cm^{-1} peak area and the contact angle versus mole fraction of **I** in the loading solution (Figs. 5 and 6). The second assumption is also supported by the data in Figs. 5 and 6, as well as by the relative invariance of the morphology of the spectra in Fig. 4 with changing surface coverage of **I**. (Large changes in orientation would lead to changes in the enhancement ratios for the various vibrational bands, depending on the directions of their dipole moment changes with respect to the surface normal¹⁰. This would change the relative intensities of the bands, which is not observed.)

Given these assumptions, one can construct a plot of δ versus normalized surface coverage (θ) by using the band positions and the 1588 cm^{-1} peak areas extracted from the spectra in Fig. 4. The normalization factor is the peak area at maximum surface coverage of I, which is obtained by extrapolating the curve in Fig. 5 to a mole fraction of 1.0. The singleton frequency was taken to be 1587 cm^{-1} , which was obtained by extrapolation of a plot of band frequency versus mole fraction of compound I to a mole fraction of zero. The plot is shown in Fig. 7. It is approximately linear up to $\theta = 0.6$, after which the values of δ deviate in the negative direction. The linearity of this plot at lower values of θ strongly suggests that the dipolar coupling model is applicable in this case. The negative deviations at high θ values are likely due to non-random occupancy of the surface sites. Deviations in this direction would be consistent with repulsive interactions between dipoles during the assembly process causing incoming dipolar species to avoid dipoles that were already present on the surface, a phenomenon that might be expected at higher θ values where the total dipolar repulsion energy would be greatest.

Linear plots of δ versus θ have been observed for several dipolar adsorbate systems³⁻⁷. However, it has been argued that this behavior does not necessarily imply that the dipolar coupling model is appropriate for a given system.¹⁰ A more convincing argument is based on a quantitative comparison of the values of $(\partial\mu/\partial Q)^2$ calculated from the experimentally observed frequency shifts using equation 1 and obtained from the integrated absorbance of the relevant spectral band. This latter quantity is obtained from the infrared spectrum of a bulk, isotropic sample using the relationship given in equation 2 below:¹⁰

$$A = \left(\frac{1}{CI} \right)_{\text{band}} \int \ln\left(\frac{I}{I_0}\right) dv = \left[\frac{\pi}{3c^2} \right] \left(\frac{\partial\mu}{\partial Q} \right)^2 \quad (2)$$

where A is the integrated absorbance of the band (in units of $\text{cm}/\text{molecule}$), C is the number concentration of molecules in the sample (in molecules per cm^3), I is the sample thickness (in cm), I and I_0 are the transmitted intensities with and without the absorber, respectively, v is the frequency (in cm^{-1}), and the other quantities have been previously defined. Use of this relationship gives $(\partial\mu/\partial Q)^2$ in the Gaussian units of $\text{esu}^2\text{ g}^{-1}$. The factor of 3 in equation 2 accounts for the random orientation of the molecules in a bulk, isotropic sample. We return to the use of this equation to obtain $(\partial\mu/\partial Q)^2$ below.

In principle, equation 1 can be used to calculate $(\partial\mu/\partial Q)^2$ from the band shift at any given surface coverage. This is most easily accomplished using the value of δ obtained by extrapolation of the plot in Fig. 7 to a θ value of 1.0, because under this condition one can use simple geometric arguments to

estimate the value of R_{av} , the average separation distance between dipolar species, from the molecular area of **I**. Using the first four points in the plot (i.e. prior to the onset of the negative deviations observed at higher θ values), this extrapolation procedure gives $\delta = 3.7 \times 10^4 \text{ cm}^{-2}$ at $\theta = 1.0$. Next, a value of M_r is required. To obtain this, we assume that the atoms that are displaced during the vibration are carbon atoms in the ring systems, so M_r , the reduced mass of the oscillator, is calculated from the molar mass of two carbon atoms. Finally, one requires an explicit value for the sum over R^{-3} for all of the dipolar species that are sufficiently close to the given dipole to significantly influence its energy. Thus, one needs both the value of R_{av} and a factor that accounts for the sum over all relevant neighbors. The first quantity is calculated from the projected molecular area of **I**, assuming closest packing at saturation surface coverage. Using molecular models, we obtain a molecular area of ca. $45\text{-}50 \text{ \AA}^2/\text{molecule}$, depending on the identity of the counterion, its position within the monolayer and the orientation of the long axis of **I**. Using a simple square lattice model, this surface coverage gives an average separation between the dipolar species of $6.7 - 7.1 \text{ \AA}$. Taking the average value of 6.9 \AA gives a value for R_{av}^{-3} of $3.3 \times 10^{-28} \text{ m}^3$. These molecular areas are consistent with our previous experience with the interfacial packing behavior of viologen groups, which have a similar size and shape and, therefore, projected area. Molecular areas for those species were determined to be in the range of $40\text{-}45 \text{ \AA}^2/\text{molecule}$.²⁸

The sum factor was obtained by iterative calculation using the number of neighbors at a given distance in each shell of the lattice. This procedure is illustrated by the following equation:

$$F = \left(\frac{n_1}{d_1^3} \right) + \left(\frac{n_2}{d_2^3} \right) + \left(\frac{n_3}{d_3^3} \right) + \dots \quad (3)$$

where F is the factor that accounts for the sum over all relevant neighbors, n_x is the number of neighbors at a given distance, d_x , and the d values are given as multiples of R_{av} (e.g. in the first shell of a square lattice, there are four neighbors at a distance of $1R_{av}$ and four at a distance of $1.41R_{av}$, etc.). Since this sum converges very slowly,¹³ its value was more conveniently obtained by plotting the intermediate values of F for each completed shell versus the reciprocal of the shell number, and extrapolating to the origin (i.e. infinite shell number). This gave a value for F of ca. 9.0. Thus, the sum over R^{-3} for all relevant neighbors in equation 1 can be replaced with F/R_{av}^{-3} , which allows explicit calculation of $(\partial\mu/\partial Q)^2$ from the value of δ extrapolated to $\theta = 1.0$. After conversion of $(\partial\mu/\partial Q)^2$ from SI to Gaussian units (for consistency with the literature), one obtains a value for $(\partial\mu/\partial Q)^2$ of $2.1 \times 10^5 \text{ esu}^2/\text{g}$. This value is characteristic of a very intense transition, which is expected based on the prominence of this band in the spectra presented above. It can be compared to the range of values of $(\partial\mu/\partial Q)^2$ for the very intense C=O

stretches of mononuclear metal carbonyl complexes of $1.2 \times 10^5 - 2.0 \times 10^5 \text{ esu}^2/\text{g}$.²⁹ Thus, this calculation of $(\partial\mu/\partial Q)^2$ from the experimentally obtained value of δ assuming a dipolar coupling model and the other assumptions discussed above produces a very reasonable value for $(\partial\mu/\partial Q)^2$.

As indicated by equation 2 above, the integrated absorbance of the 1588 cm^{-1} band also provides a measure of $(\partial\mu/\partial Q)^2$. The integrated absorbance for the 1588 cm^{-1} band was for a sample of known quantity in a KBr pellet, giving a value of $2.8 \times 10^{-16} \text{ cm}/\text{molecule}$. Use of this quantity in equation 2 gives a value for $(\partial\mu/\partial Q)^2$ of $2.4 \times 10^5 \text{ esu}^2/\text{g}$. Given the number of assumptions involved in obtaining $(\partial\mu/\partial Q)^2$ from equation 1, these values are in excellent agreement. This very strongly suggests that the spectral shifts observed for this band are, indeed, due to a through-space, electrostatic dipole-dipole coupling interaction between the stilbazolium derivatives in the monolayer.

This dipolar coupling analysis was not applied to the 1528 cm^{-1} band because the small spectral shifts that were observed for this band precluded the extraction of quantitative data for this case. However, it is worth noting that the considerably lower intensity of this band compared to the 1588 cm^{-1} band, which implies a smaller value for $(\partial\mu/\partial Q)^2$ according to equation 2, suggests that the coupling should be much smaller. In fact, if one assumes that the intensity ratio of the 1528 cm^{-1} and 1588 cm^{-1} bands can be used to obtain a measure of $(\partial\mu/\partial Q)^2$ for the 1528 cm^{-1} band, the value obtained for $(\partial\mu/\partial Q)^2$ is ca. $0.3 \times 10^5 \text{ esu}^2/\text{g}$. Using equation 1, this predicts a maximum shift (i.e. from zero to saturation surface coverage) for this band due to dipolar coupling of ca. 1 cm^{-1} . This is at least in qualitative agreement with observations. Further, on inspection of the calculated atomic displacements during the vibrations assigned to the 1528 cm^{-1} and 1588 cm^{-1} bands (Fig. 3), it seems intuitively reasonable that the value of $(\partial\mu/\partial Q)^2$ would be larger for the the 1588 cm^{-1} band, since it might be expected that ring-based stretches would lead to larger charge oscillation between the rings than would stretches of the C-C bonds between the vinyl group and the two rings.

Finally, we note in passing that the influence image dipoles in the metal on the vibrational frequencies of adsorbates has been discussed extensively.^{4,15,30} Briefly, this effect is due to the self-image from the oscillating dipole near a metal surface. It should be independent of surface coverage (to a first approximation) and always results in a *lowered* frequency for the band. Also, theoretical models⁴ for this effect imply a very strong (cubic) dependence of the shift on the distance of the dipole from the surface. There are two points to consider in determining the relevance of this effect to our results. First, in our case, the dipolar species is much farther from the surface than for other cases where the effect has been argued to be significant. For example, for CO adsorbed on Pt surfaces, the distance is typically taken to be ca. 1 \AA ,⁴ while in our case the center of the dipole is ca. 8 \AA from the surface, based on molecular models

and assuming an orientation parallel to the surface normal. This dramatic increase in distance should certainly decrease the magnitude of the effect. Second, since the effect is (to first order) independent of surface coverage, it should not affect the value of δ , so it should have no influence on our calculations of $(\partial\mu/\partial Q)^2$. Thus, we have neglected such effects in our treatment of the data presented above.

Conclusions

To our knowledge, these results comprise the first unambiguous report of through-space, electrostatic dipolar coupling between adsorbates. The fact that the experiments were done under conditions where the adsorbates cannot achieve direct contact with the metal precludes the possibility of vibrational (i.e. inductive) coupling of the type described by Moskovits and Hulse.¹⁰ Further, the very good agreement between the values of $(\partial\mu/\partial Q)^2$ obtained from the experimental band shifts using the dipolar coupling model and the integrated absorbance of the 1588 cm^{-1} band provides additional, strong support for the notion that dipolar coupling is the dominant effect in this system.

This experimental system provides an excellent example of the power of the self-assembly method for producing interfacial assemblies whose structure can be controlled sufficiently to manipulate the properties of species within the assembly. A particularly interesting and topical area for such studies relates to the use of self-assembly methods to produce materials that exhibit large non-linear optical (NLO) effects.³¹ In these applications, detailed knowledge of the effect of the environment on the properties of chromophoric moieties within the material will undoubtedly prove to be the ultimate success of these endeavors. For example, recent work by Marks and coworkers indicates that intermolecular dipole-dipole interactions can have a significant influence on the hyperpolarizability of the chromophore, leading to relatively large changes in second harmonic generation from the material.³² Their results suggest that ways to both control and measure dipole-dipole interactions in such assemblies will be useful in understanding the NLO properties of these material.

Acknowledgements

We are grateful to the Office of Naval Research for the full support of this work.

References

1. Ulman, A. *An Introduction to Ultrathin Organic Films: From Langmuir-Blodgett to Self-Assembly*; Academic Press: Boston, 1991.
2. Pope, J. M.; Tan, Z.; Kimbrell, S.; Buttry, D. A. *J. Am. Chem. Soc.* **1992**, *114*, 10085-86.
3. For a recent example, see Paul, D. K.; Beebe, T. P., Jr.; Uram, K. J.; Yates, J. T., Jr. *J. Am. Chem. Soc.* **1992**, *114*, 1949-54.

4. Willis, R. F.; Lucas, A. A.; Mahan, G. D. *The Chemical Physics of Solid Surfaces and Heterogeneous Catalysis*; King, D. A., Woodruff, D. P., Eds.; Vol. 2, pp 67-100.
5. Yates, J. T., Jr. *Surf. Sci.* **1994**, *299/300*, 731-741.
6. a.) Kim, C. S.; Tornquist, W. J.; Korzeniewski, C. *J. Chem. Phys.* **1994**, *101*, 9113-21. b.) Chang, S. -C.; Weaver, M. J. *J. Phys. Chem.*, **1991**, *95*, 5391-5400.
7. For similar phenomena in adsorbates other than CO, see a.) Gao, P.; Weaver, M. J. *J. Phys. Chem.*, **1989**, *93*, 6205-11. and b.) Zenobi, R.; Xu, J.; Yates, J. T., Jr.; Persson, B. N. J.; Volokitin, A. I. *Chem. Phys. Lett.*, **1993**, *208*, 414-9, and references therein.
8. Grimley, T. B. *Proc. Phys. Soc.*, **1962**, *79*, 1203.
9. Cotton, F. A.; Kraihanzel, C. S. *J. Am. Chem. Soc.*, **1962**, *84*, 4432-8.
10. Moskovits, M.; Hulse, J. E. *Surf. Sci.* **1978**, *78*, 397-418.
11. a.) Eischens, R. P.; Francis, S. A.; Pliskin, W. A. *J. Phys. Chem.* **1956**, *60*, 194-201. b.) Eischens, R. P.; Pliskin, W. A. *Adv. Catal.* **1958**, *10*, 1-56.
12. a.) Decius, J. C. *J. Chem. Phys.* **1954**, *22*, 1941-. b.) Decius, J. C. *J. Chem. Phys.* **1954**, *22*, 1946-. c.) Decius, J. C. *J. Chem. Phys.* **1955**, *23*, 1290- .
13. Hammaker, R. M.; Francis, S. A.; Eischens, R. P. *Spectrochim. Acta* **1965**, *21*, 1295-1309.
14. Mahan, G. D.; Lucas, A. A. *J. Chem. Phys.*, **1978**, *68*, 1344-8.
15. Scheffler, M. *Surf. Sci.* **1979**, *81*, 562-70.
16. Sorbello, R. S. *Phys. Rev. B* **1985**, *32*, 6294-301.
17. Olsen, C. W.; Masel, R. I. *Surf. Sci.*, **1988**, *201*, 444-60.
18. a.) Hassner, A.; Birnbaum, D.; Loew, L. M. *J. Org. Chem.*, **1984**, *49*, 2546-51. b.) Alternately, given in Kost, A. N.; Sheinkman, A. K.; Rozenberg, A. N. *J. Gen. Chem. USSR (Engl. Transl.)*, **1964**, *34*, 4106.
19. Bain, C. D.; Troughton, E. B.; Tao, Y.-T.; Evall, J.; Whitesides, G. M.; Nuzzo, R. G. *J. Am. Chem. Soc.*, **1989**, *111*, 321-35.
20. Walczak, M. M.; Chung, C.; Stole, S. M.; Widrig, C. A.; Porter, M. D. *J. Am. Chem. Soc.* **1991**, *113*, 2370-78.
21. Shibasaki, K.; Itoh, K. *J. Raman Spectr.*, **1991**, *22*, 753-8.
22. Stroeve, P.; Saperstein, D. D.; Rabolt, J. F. *Thin Solid Films*, **1989**, *179*, 529-34.
23. Su, W. -F. A.; Kurata, T.; Nobutoki, H.; Koezuka, H. *Langmuir*, **1992**, *8*, 915-9.
24. Ziolo, R. F.; Gunther, W. H. H.; Meredith, G. R.; Williams, D. J.; Troup, J. M. *Acta Cryst.*, **1982**, *B38*, 341-43
25. Snyder, R. G.; Strauss, H. L.; Elliger, C. A. *J. Phys. Chem.*, **1982**, *86*, 5145-50.
26. Laibinis, P. E.; Whitesides, G. M.; Allara, D. L.; Tao, Y. -T.; Parikh, A. N.; Nuzzo, R. G. *J. Am. Chem. Soc.*, **1991**, *113*, 7152-67.

27. Rowe, G. K.; Creager, S. E. *Langmuir*, **1991**, *7*, 2307-12.
28. De Long, H. C.; Buttry, D. A. *Langmuir*, **1992**, *8*, 2491-96.
29. Darensbourg, D. J.; Brown, T. L. *Inorg. Chem.*, **1968**, *7*, 959-65.
30. Persson, B. N. *J. Solid State Commun.* **1978**, *27*, 417-21.
31. a.) Katz, H. E.; Scheller, G.; Putvinski, T. M.; Schilling, M. L.; Wilson, W. L.; Chidsey, C. E. D. *Science*, **1991**, *254*, 1485-7. b.) Schilling, M. L.; Katz, H. E.; Stein, S. M.; Shane, S. F.; Wilson, W. L.; Buratto, S.; Ungashe, S. B.; Taylor, G. N.; Putvinski, T. M.; Chidsey, C. E. D. *Langmuir*, **1993**, *9*, 2156-60. c.) Li, D.; Ratner, M. A.; Marks, T. J.; Zhang, C.; Yang, J.; Wong, G. K. *J. Am. Chem. Soc.*, **1990**, *112*, 7389-90. d.) Roscoe, S. B.; Yitzchaik, S.; Kakkar, A. K.; Marks, T. J.; Lin, W.; Wong, G. K. *Langmuir*, **1994**, *10*, 1337-39. e.) Evans, C. E.; Bohn, P. W. *J. Am. Chem. Soc.*, **1993**, *115*, 3306-11.
32. a) Di Bella, S.; Ratner, M. A.; Marks, T. J. *J. Am. Chem. Soc.*, **1992**, *114*, 5842-49, b) Di Bella, S.; Fragala, I. L.; Ratner, M. A.; Marks, T. J. *J. Am. Chem. Soc.*, **1993**, *115*, 682-86.

Table I - Vibrational assignments for compound I

vibrational band frequency, cm ⁻¹	assigned mode	general orientation of mode
1176	aliphatic C-N stretch aliphatic C-N stretch	to long axis to long axis
1528	vinylic C-C stretch ^a	to long axis
1588	vinylic C=C stretch benzene ring stretch coupled ring displacements ^c	54° off long axis ²⁴ to long axis to long axis
1600	benzene ring stretch aromatic C=C stretch	⊥ to long axis to long axis
1640	vinylic C=C stretch vinylic C=C stretch ^d	54° off long axis 54° off long axis

^a This mode is graphically depicted in Figure 3a.

^b Assigned from SERRS spectra.

^c This mode is graphically depicted in Figure 3b.

^d This mode is graphically depicted in Figure 3c.

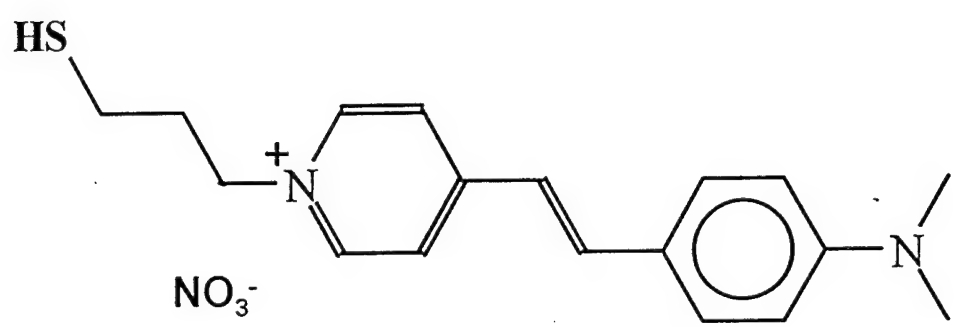
Table II - Vibrational assignments for alkyl chains

<u>vibrational band frequency, cm⁻¹</u>	<u>assigned mode</u>	<u>general orientation of mode</u>
2850	symmetric CH ₂ stretch	in HCH plane, ⊥ to chain
2878	symmetric CH ₃ stretch	to C-CH ₃ bond
2919	asymmetric CH ₂ stretch	⊥ to CCC backbone plane
2964	asymmetric CH ₃ stretch, in plane	in plane of CCC backbone, ⊥ to C-CH ₃ bond

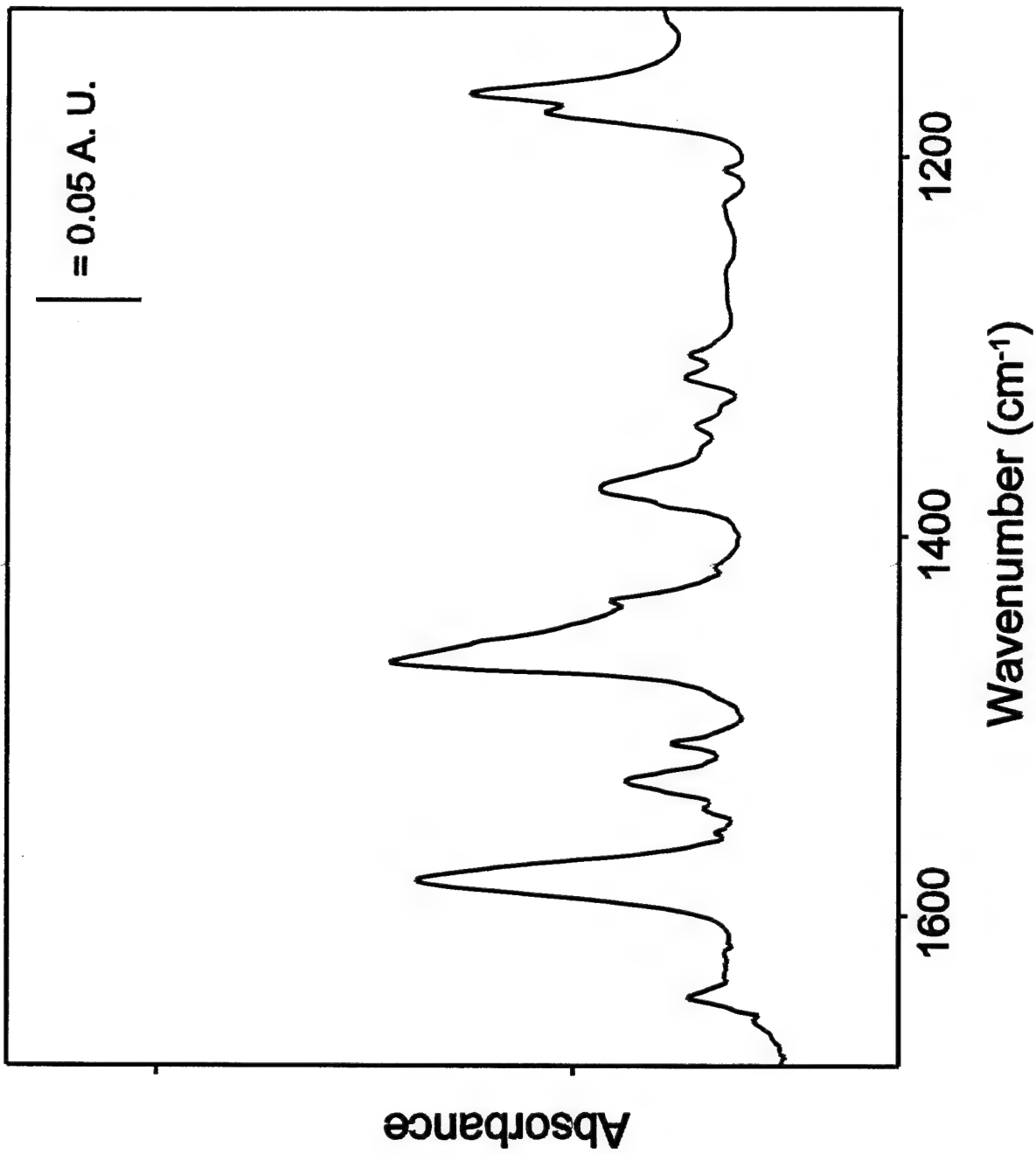
All assignments and orientations were taken from refs. 25 and 26.

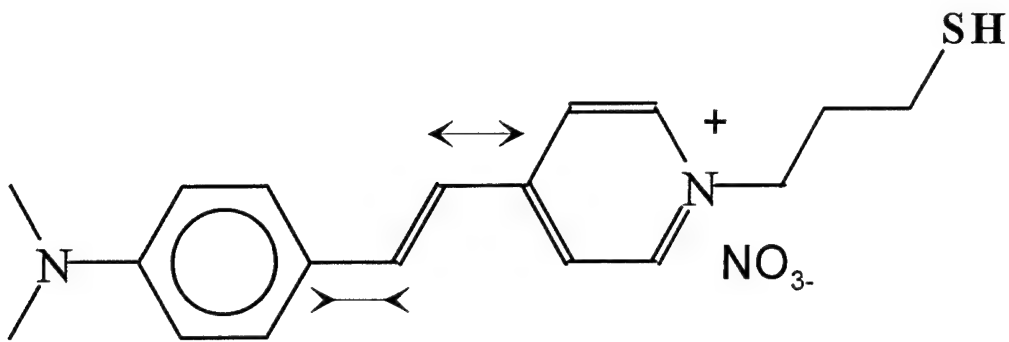
Figure captions

1. Structure of compound I.
2. Transmission infrared spectrum of a bulk sample of compound I.
3. Illustration of the calculated, predominant atomic displacements during vibration for the 1528, 1588, and 1640 cm^{-1} bands.
4. RA-FTIR spectra in the ring stretching region (plate A) and in the CH stretching region (plate B) for six different SAM's prepared at several mole fractions of compound I in the loading solutions. Spectra a-f in each plate correspond to mole fractions of compound I of 0.1, 0.2, 0.5, 0.8, 0.9, and 0.95, respectively.
5. Plots of the peak areas of the 2850 and 1588 cm^{-1} bands (in cm^{-1}) versus the mole fraction of compound I in the loading solutions.
6. Plot of the advancing contact angle of water on the SAM's versus the mole fraction of compound I in the loading solutions.
7. Plot of δ versus normalized peak area for the 1588 cm^{-1} band. See text for details.

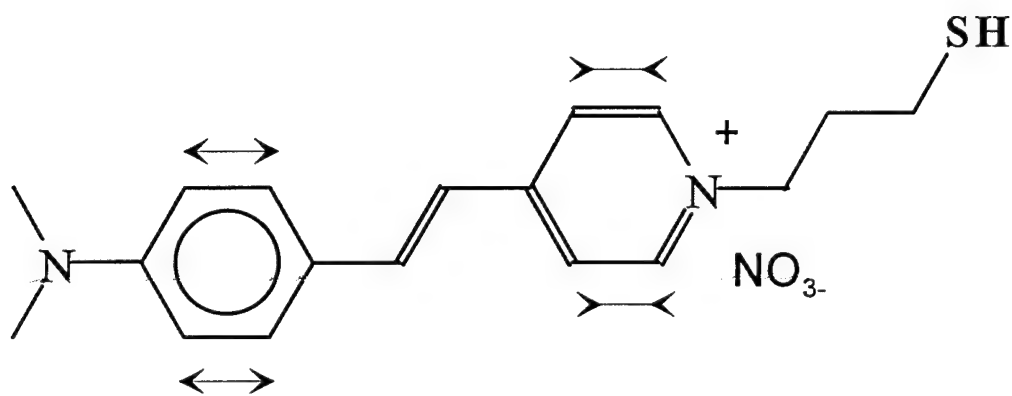


(1)

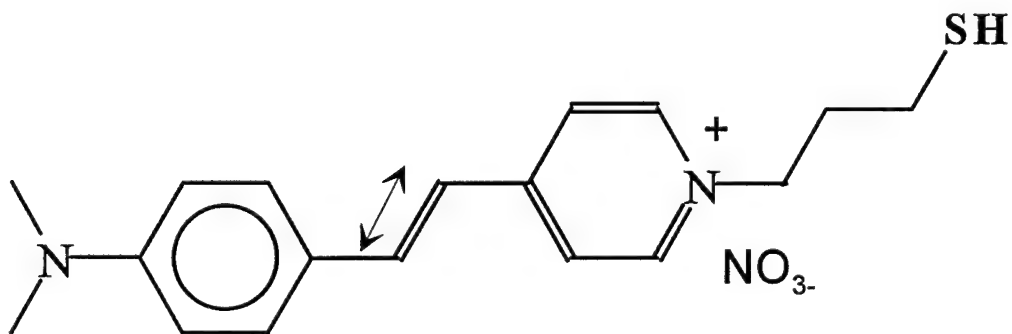




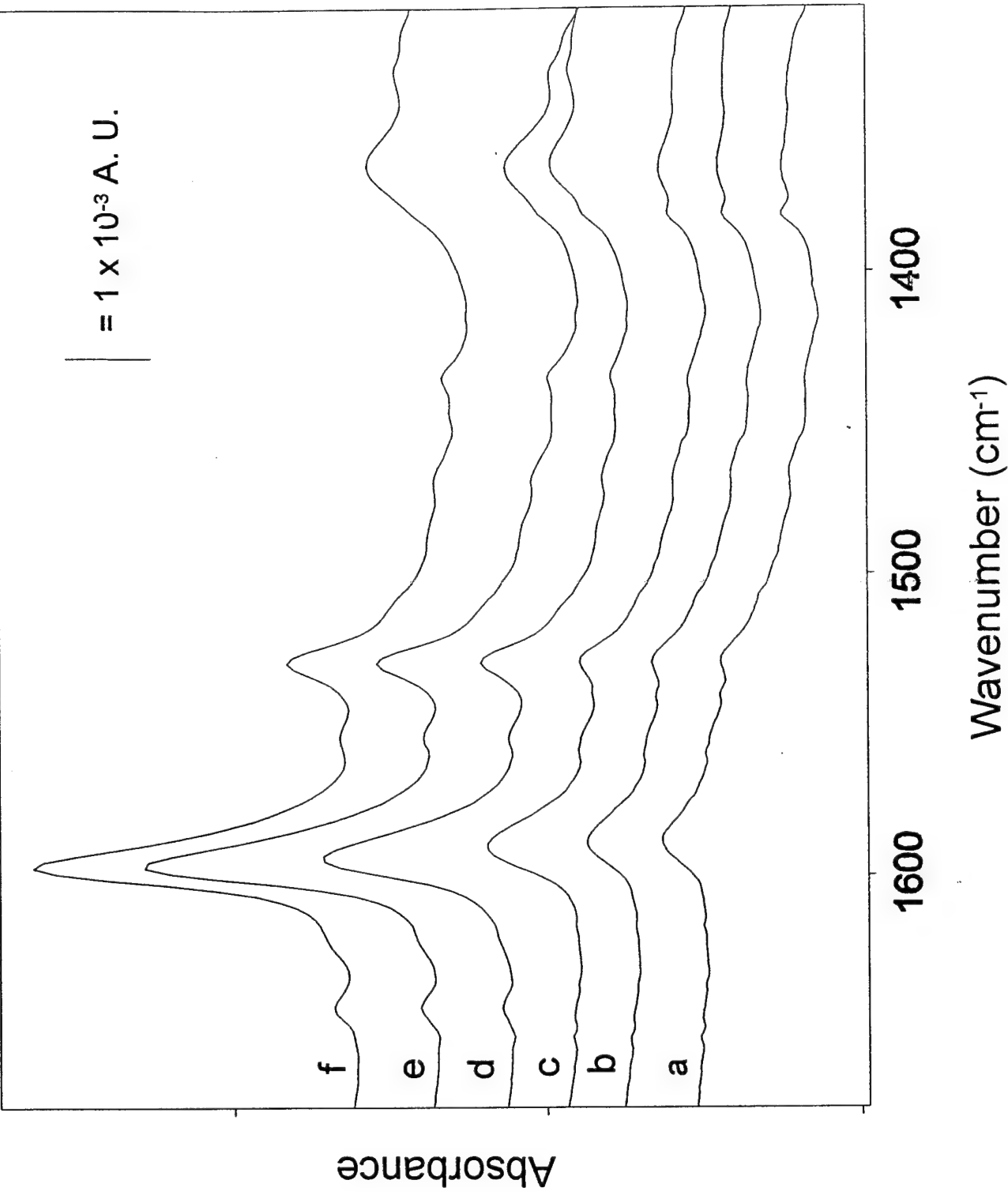
A. Primary bond contributions to the 1528 cm^{-1} band



B. Primary bond contributions to the 1588 cm^{-1} band



C. Primary bond contributions to the 1640 cm^{-1} band



β Cm / if

